Supporting Information

Ortho-π-extension of perylene diimides via one-pot annulation of imidazo[1,2-a]pyridine or imidazo[1,2-a]pyrazine for n-type organic field-effect transistors

Yinxiang Liao,[a] Cui Wang,[a] Luyao Dai,[a] Guangwei Shao,[b] Xingyu Chen,[c] Di Wu,*[a],[b] and Jianlong Xia*[a],[b],[c]

[a] School of Chemistry, Chemical Engineering and Life Science, Wuhan University of Technology, No. 122 Luoshi Road, Wuhan 430070, China

[b] State Key Laboratory of Advanced Technology for Materials Synthesis and Processing, Center of Smart Materials and Devices, Wuhan University of Technology, No. 122 Luoshi Road, Wuhan 430070, China

[c] International School of Materials Science and Engineering, Wuhan University of Technology, No. 122 Luoshi Road, Wuhan, 430070, China

*Corresponding authors：

E-mail: D.W. (chemwd@whut.edu.cn); J.X. (jlxia@whut.edu.cn)

General information

^{1}H NMR and ^{13}C NMR spectra were measured on Bruker Avance IIIHD. MALDI-TOF Mass spectrum was measured with AB Sciex 5800. UV-vis spectrum was recorded on Shimadzu UV-1800, while photoluminescence emission spectra were obtained using a Shimadzu RF-6000 fluorescence spectrometer. Cyclic voltammograms (CVs) were obtained on CHI660E electrochemical workstation. A three-electrode one-compartment cell containing a solution of the analyte and supporting electrolyte (tetrabutylammonium, ($[NBu_4]PF_6$), 0.1 M) in dry CH_2Cl_2 was utilized. The three-electrode were a 500 μm diameter platinum-disk as working electrode, a platinum-wire as counter electrode, and an Ag/AgCl as reference electrode. The measurements were obtained under a scanning rate of 100 mV/s. Thermogravimetric analysis (TGA) was performed on a TA Instruments SDT Q-600 under a nitrogen atmosphere at a heating rate of 10 °C/min. X-ray diffraction (XRD) data were collected on a Bruker AXS D8 diffractometer using Cu Kα radiation. All XRD samples were spin-coated onto appropriate substrates prior to analysis.

Material synthesis

Compound **PDI-IPD**: Under a nitrogen atmosphere, perylene diimide derivative **I** (100 mg, 0.01 mmol) was reacted with aminopyridine (28 mg, 0.30 mmol), potassium tert-butanolate (68 mg, 0.61 mmol), and Pd(dppf)Cl_2 (11 mg, 0.015 mmol) in 40 mL toluene at 100 °C for 3 h. After cooling to room temperature, the reaction mixture was concentrated under reduced pressure to remove the solvent. The crude product was purified by silica gel column chromatography (eluent was petroleum ether : dichloromethane = 1:3) and recrystallized from dichloromethane and methanol, affording a turquoise solid (33 mg, 32.62%).

^{1}H NMR (500 MHz, Chloroform-*d*) δ 10.28 (d, *J* = 8.3 Hz, 1H), 10.11 (d, *J* = 7.3 Hz, 1H), 8.36-8.32 (m, 2H), 8.25 (d, *J* = 7.7 Hz, 1H), 8.16 (d, *J* = 8.1 Hz, 1H), 8.12 (d, *J* = 8.1 Hz, 1H), 7.57-7.51 (m, 2H), 6.83 (t, *J* = 6.6 Hz, 1H), 4.14 (d, *J* = 7.4 Hz, 2H), 4.08 (d, *J* = 7.4 Hz, 2H), 2.07-1.96 (m, 3H), 1.33-1.18 (m, 65H), 0.83 (q, *J* = 6.9, 6.4 Hz, 13H).

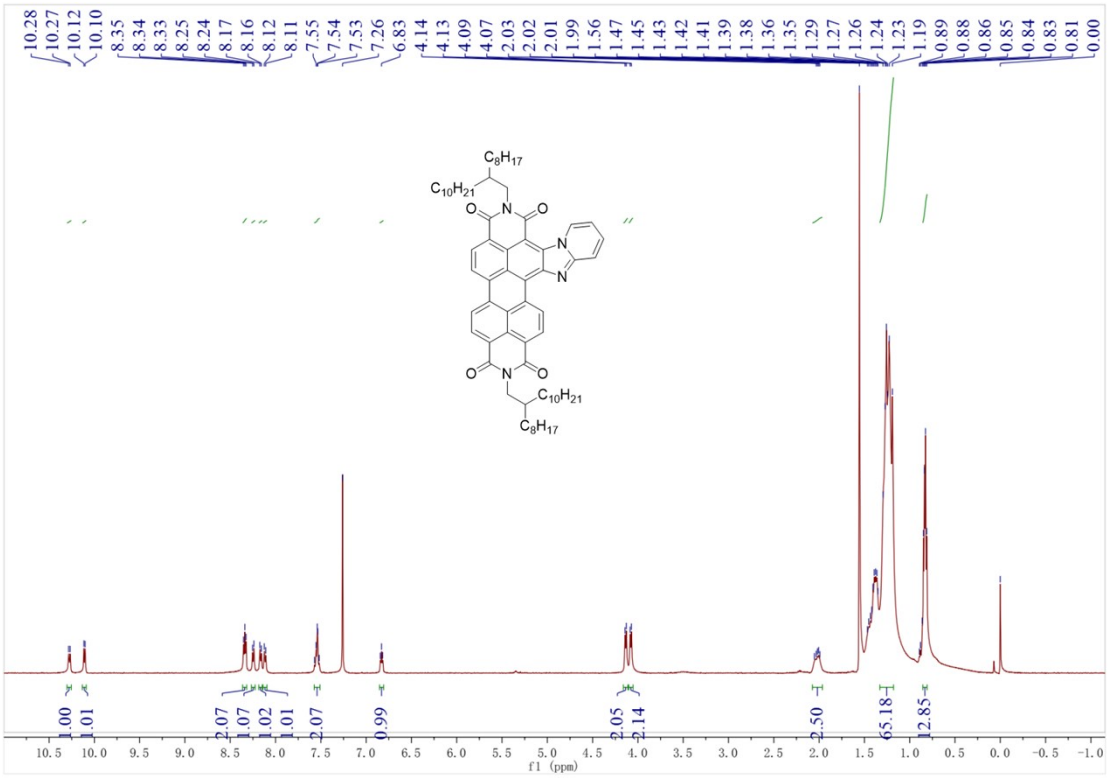

Figure S1. ^{1}H NMR spectroscopy of **PDI-IPD**.

^{13}C NMR (126 MHz, $CDCl_3$-*d*) δ 163.5, 163.4, 162.8, 162.6, 152.5, 143.4, 133.5, 133.4, 133.2, 133.0, 132.3, 131.1, 130.7, 129.5, 129.3, 127.8, 125.4, 124.3, 123.2, 123.0, 122.4, 121.8, 121.7, 121.4, 120.9, 117.6, 110.6, 109.1, 44.7, 37.0, 36.7, 31.94, 31.93, 31.90, 31.8, 31.7, 30.22, 30.20, 29.74, 29.71, 29.69, 29.66, 29.38, 29.37, 29.3, 26.6, 26.5, 22.68, 22.66, 22.6, 14.08, 14.05, 14.0.

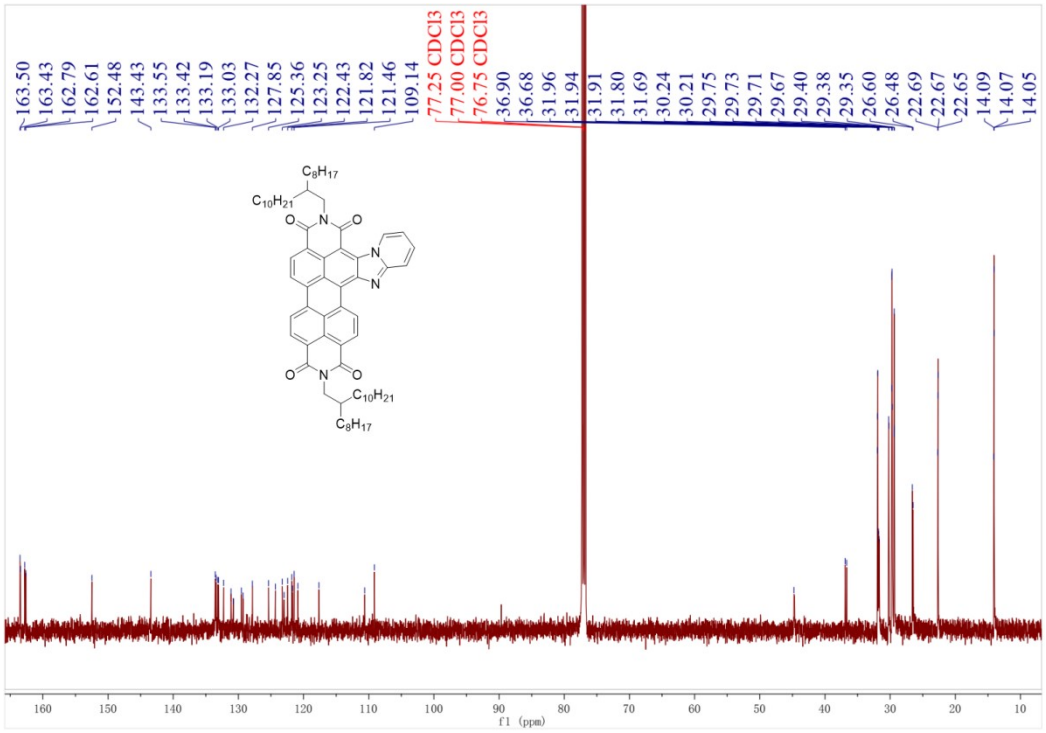

Figure S2. ^{13}C NMR spectroscopy of **PDI-IPD**.

$[M+H]^+$ MALDI-TOF MS: calculated for 1041.7197; found 1041.7185.

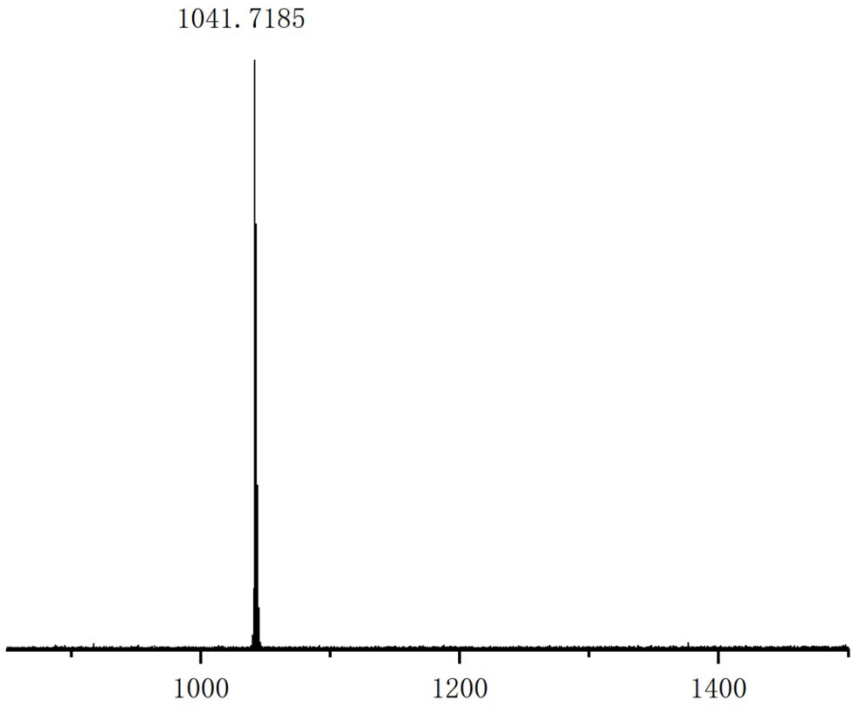

Figure S3. MALDI-TOF spectrum of compound **PDI-IPD**

Compound **PDI-IPZ**: Under a nitrogen atmosphere, perylene diimide derivative

I (100 mg, 0.01 mmol) was reacted with aminopyrazine (28 mg, 0.30 mmol), potassium tert-butanolate (68 mg, 0.61 mmol), and Pd(dppf)Cl_2 (11 mg, 0.015 mmol) in 40 mL toluene at 100 °C for 3 h. After cooling to room temperature, the reaction mixture was concentrated under reduced pressure to remove the solvent. The crude product was purified by silica gel column chromatography (eluent was dichloromethane) and recrystallized from dichloromethane and methanol, affording a turquoise solid (40 mg, 39.50%).

^{1}H NMR (500 MHz, Chloroform-*d*) δ 10.39 (d, *J* = 8.2 Hz, 1H), 10.16 (d, *J* = 5.1 Hz, 1H), 9.26 (s, 1H), 8.48 (d, *J* = 7.8 Hz, 1H), 8.44 (dd, *J* = 8.1, 6.0 Hz, 2H), 8.31 (dd, *J* = 8.4, 2.6 Hz, 2H), 8.00 (d, *J* = 5.0 Hz, 1H), 4.14 (d, *J* = 7.3 Hz, 4H), 2.03 (s, 2H), 1.25 (dd, *J* = 19.6, 8.5 Hz, 64H), 0.85-0.82 (m, 13H).

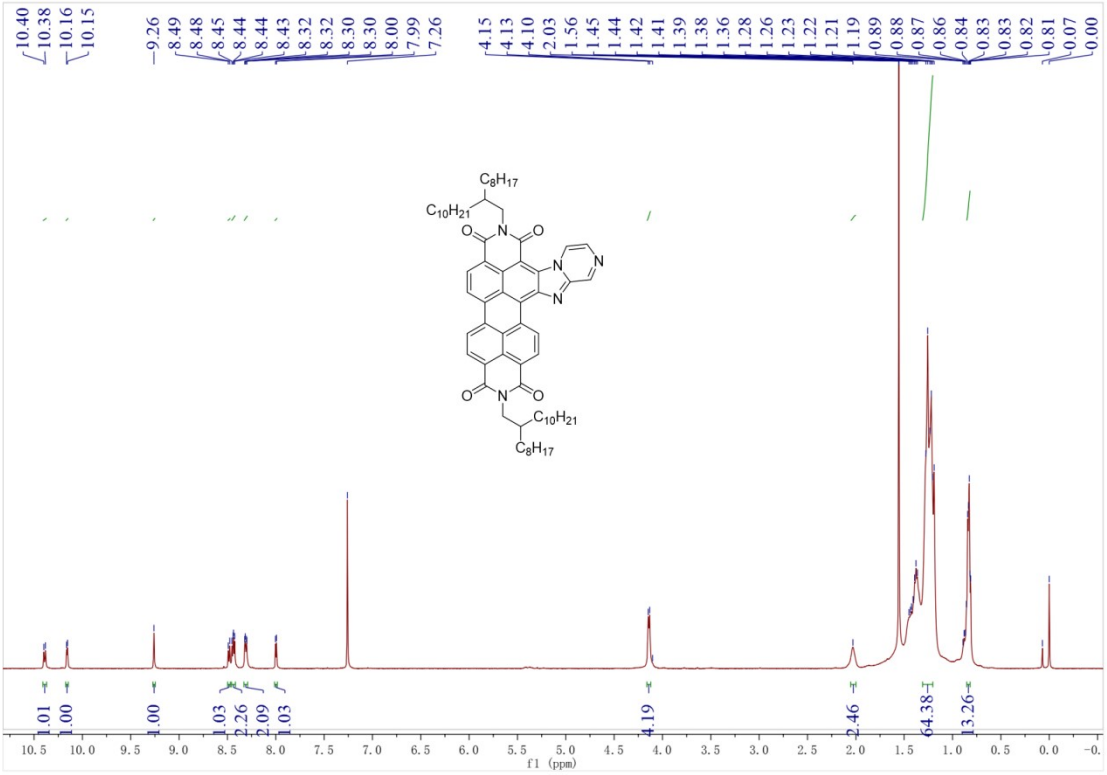

Figure S4. ^{1}H NMR spectroscopy of **PDI-IPZ**.

^{13}C NMR (126 MHz, $CDCl_3$-*d*) δ 163.5, 163.4, 162.8, 162.6, 152.5, 143.4, 133.6, 133.4, 133.2, 133.0, 132.3, 131.1, 130.8, 129.5, 129.3, 127.9, 125.4, 124.3, 123.3, 123.0, 122.4, 121.8, 121.7, 121.5, 120.9, 117.6, 110.6, 109.1, 44.8, 36.9, 36.7, 31.96, 31.94, 31.9, 31.8, 31.7, 30.24, 30.21, 29.8, 29.73, 29.71, 29.7, 29.40, 29.38, 29.35, 26.6, 26.5, 22.69, 22.67, 22.65, 14.09, 14.07, 14.05.

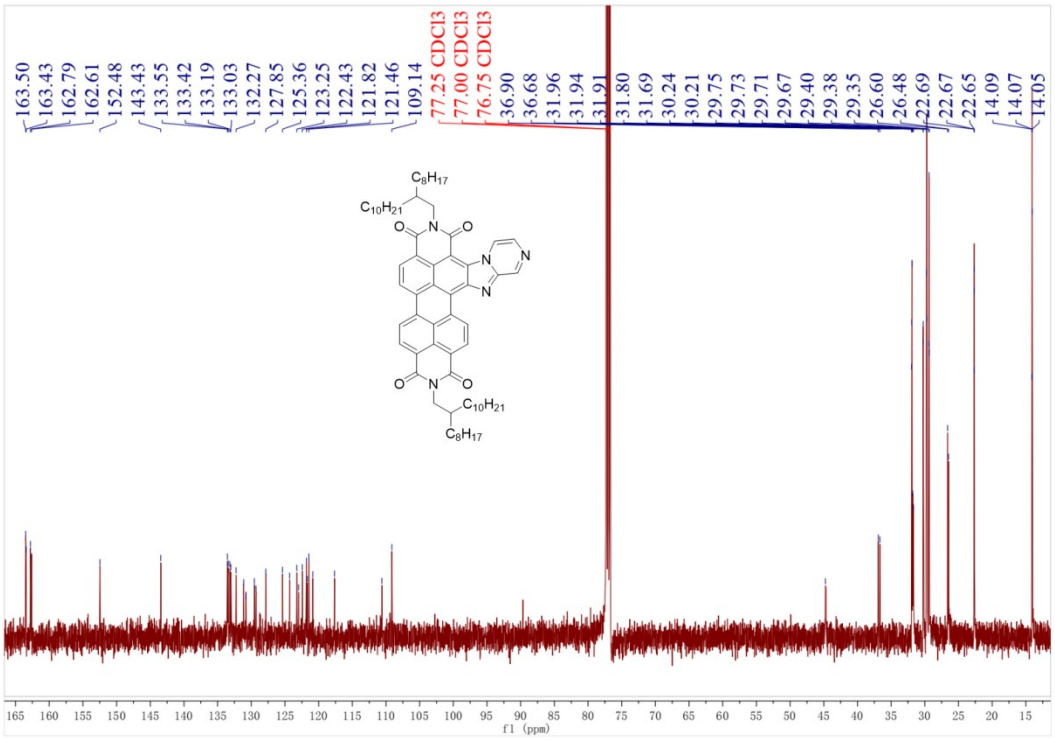

Figure S5. ^{13}C NMR spectroscopy of PDI-IPZ.

$[M+H]^+$ MALDI-TOF MS: calculated for 1042.7149; found 1042.7135.

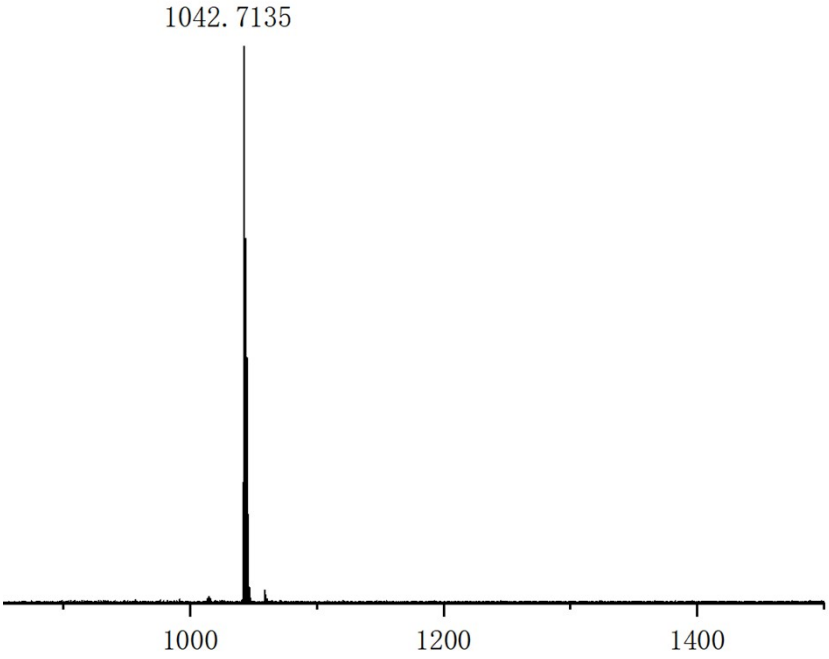

Figure S6. MALDI-TOF spectrum of compound **PDI-IPZ**

DFT calculation

Table S1. DFT optimized the HOMO and LUMO of **PDI-IPD** and **PDI-IPZ**

Compound	E_{HOMO}^{cal}/eV	E_{LUMO}^{cal}/eV	E_g^{cal}/eV
PDI-IPD	−5.49	−3.41	2.09
PDI-IPZ	−5.71	−3.62	2.09

The fabrication of OFET devices

Bottom-gate top-contact (BGTC) organic field-effect transistors (OFETs) were fabricated utilizing **PDI-IPD** and **PDI-IPZ** as semiconductor materials. The process began with the application of 5 mg ml^{-1} chloroform solution of **PDI-IPD** and **PDI-IPZ** onto an octadecyl trichlorosilane (OTS)-modified SiO_2/Si substrate, which had been optimized to achieve a thin film thickness of 20-30 nm. Following the spin-coating step, the thin films were subjected to annealing for a duration of 10 minutes at various temperatures within glovebox environment. This step was crucial for optimizing the film's morphology and molecular ordering. Subsequently, gold source and drain electrodes were evaporated and settled onto the semiconductor layer, thereby completing the device fabrication.

Thermo gravimetric analyzer (TGA)

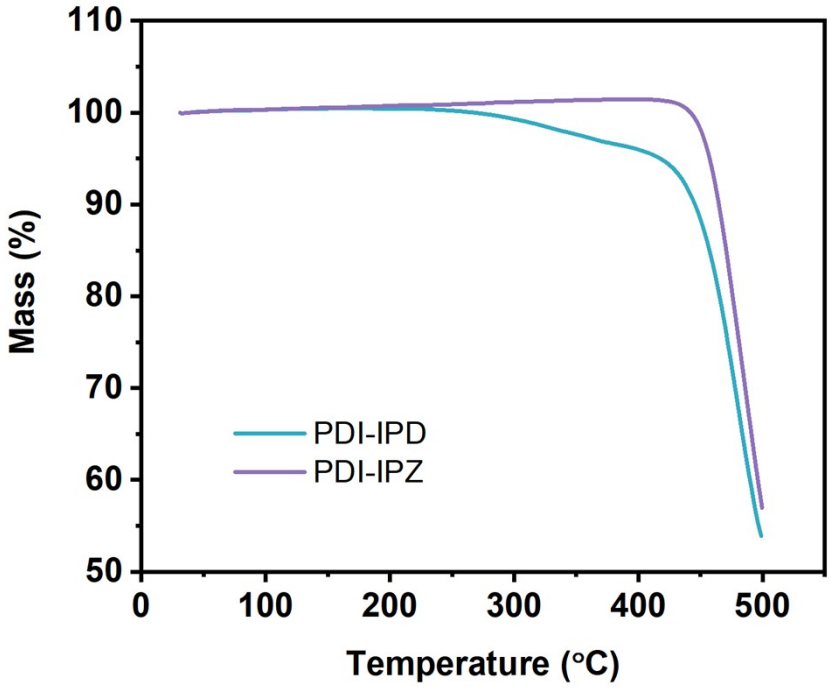

Figure S7. TGA weight loss profiles of **PDI-IPD** and **PDI-IPZ**.

The organic field-effect transistors (OFETs) performance of the devices

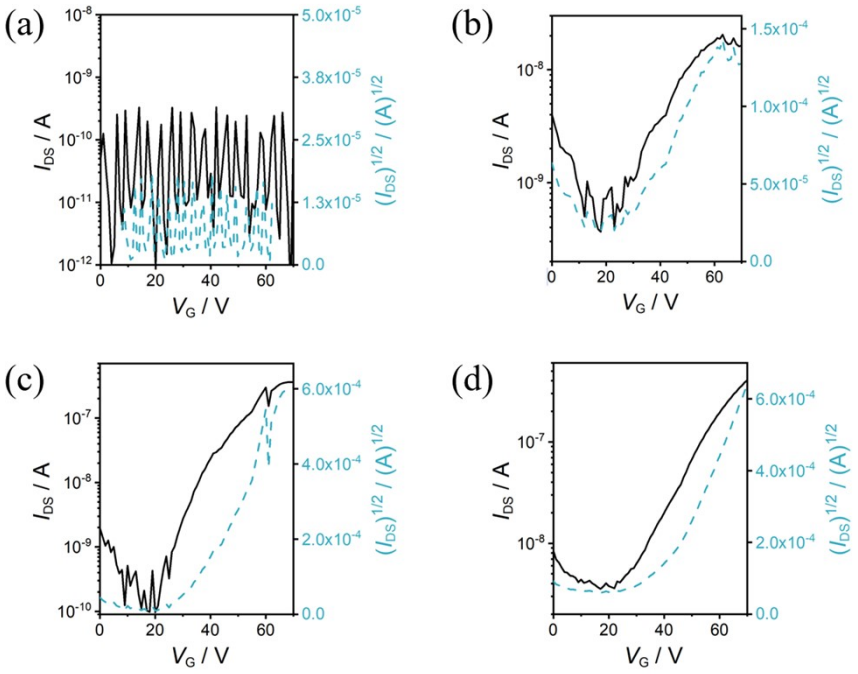

Figure S8. Transfer curves of OFETs based on **PDI-IPD** at different annealing temperature for 10 min. a, As-cast; b, 40 ℃; c, 80 ℃; d, 120 ℃.

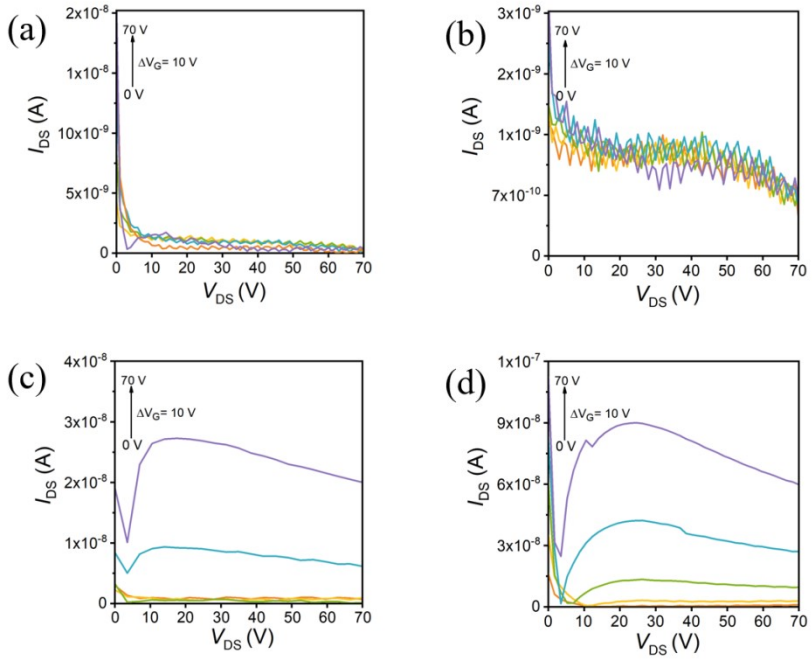

Figure S9. Output curves of OFETs based on **PDI-IPD** at different annealing temperature for 10 min, a, As-cast; b, 40 ℃; c, 80 ℃; d, 120 ℃.

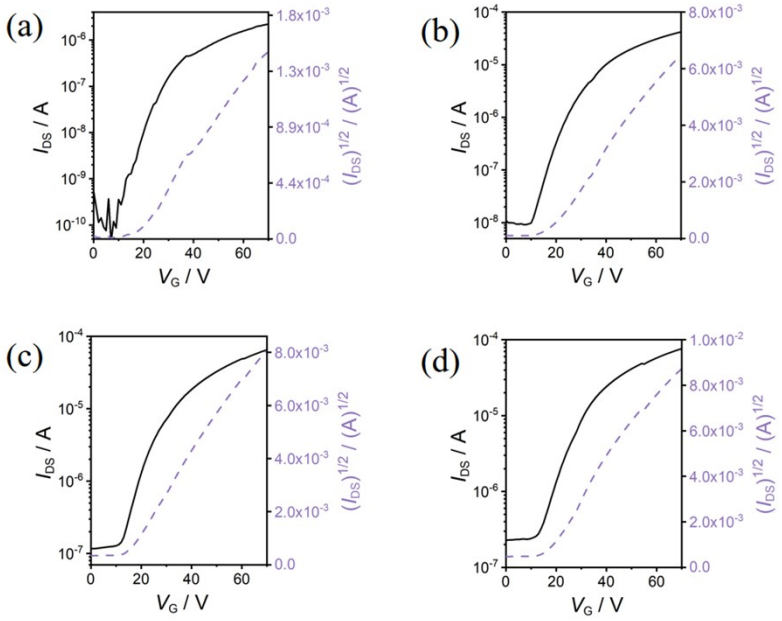

Figure S10. Transfer curves of OFETs based on **PDI-IPZ** at different annealing temperature for 10 min. a, As-cast; b, 40 ℃; c, 80 ℃; d, 120 ℃.

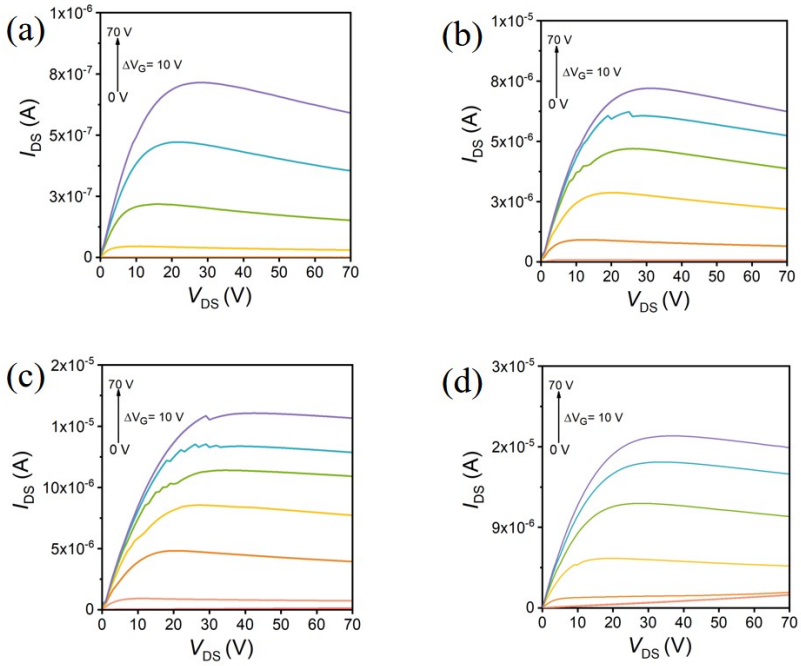

Figure S11. Output curves of OFETs based on **PDI-IPZ** at different annealing temperature for 10 min, a, As-cast; b, 40 ℃; c, 80 ℃; d, 120 ℃.

Table S2. The OFET performance of **PDI-IPD**.

Compound	Annealing Temperature (℃)	μ (cm^2 V^{-1} s^{-1})	V_{th}	I_{on}/I_{off}
PDI-IPD	As	0	0	0
	40	4.50×10^{-5}	23	10^2
	80	3.90×10^{-4}	31	10^3
	As-120 (Step annealing)	6.50×10^{-4}	36	10^2

Table S3. The OFET performance of **PDI-IPZ**.

Compound	Annealing Temperature (℃)	μ (cm^2 V^{-1} s^{-1})	V_{th}	I_{on}/I_{off}
PDI-IPZ	As	1.80×10^{-2}	18	10^4
	40	3.40×10^{-2}	20	10^3
	80	5.20×10^{-2}	15	10^3
	As-120 (Step annealing)	1.16×10^{-1}	17	10^3

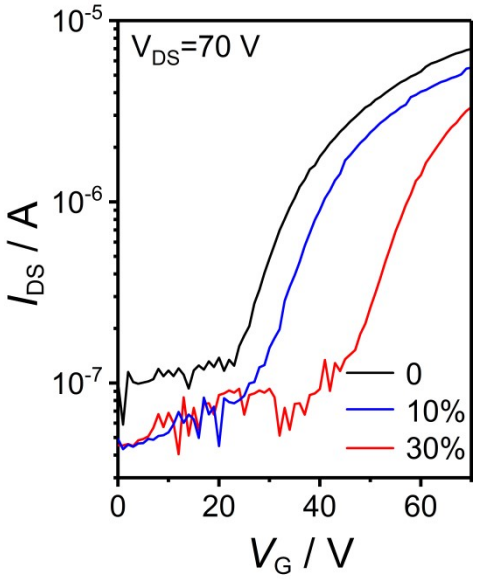

Figure S12. Transfer curves based on the **PDI-IPZ** at different humidity levels

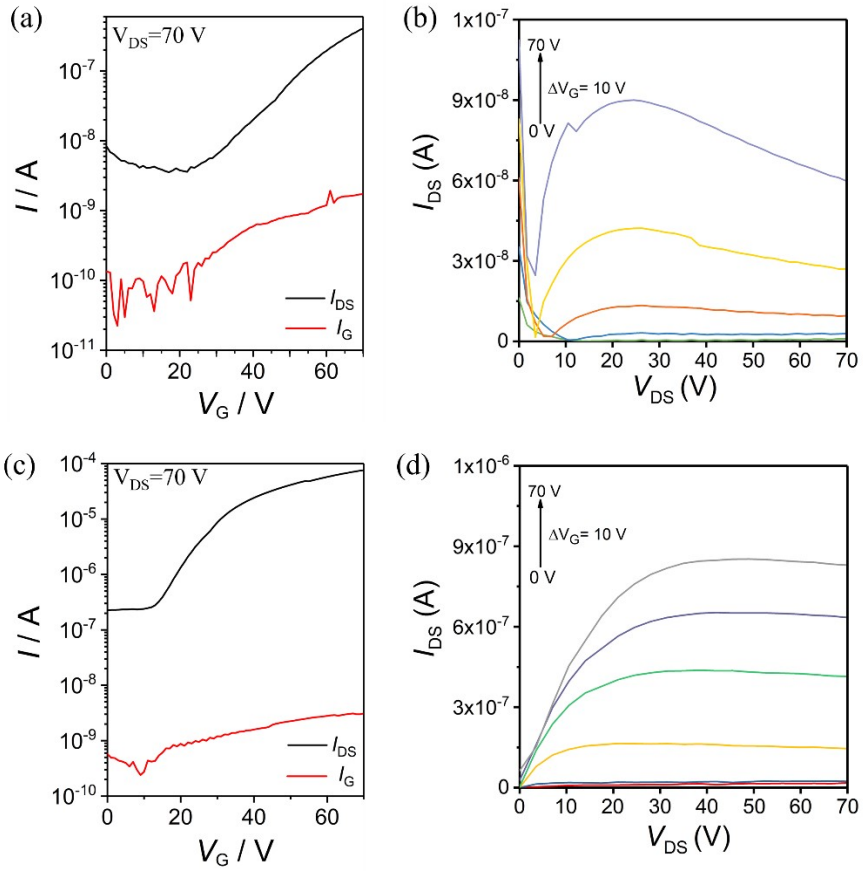

Figure S13. The drain current and the gate current at the drain voltage of 70 V as a function of gate voltage based on the **PDI-IPD** (a) and **PDI-IPZ** (c). Black and red curves represent the drain current and the gate current, respectively. Output curves of OFETs based on **PDI-IPD** (b) and **PDI-IPZ** (d).

Microscopic morphology characterizations (AFM)

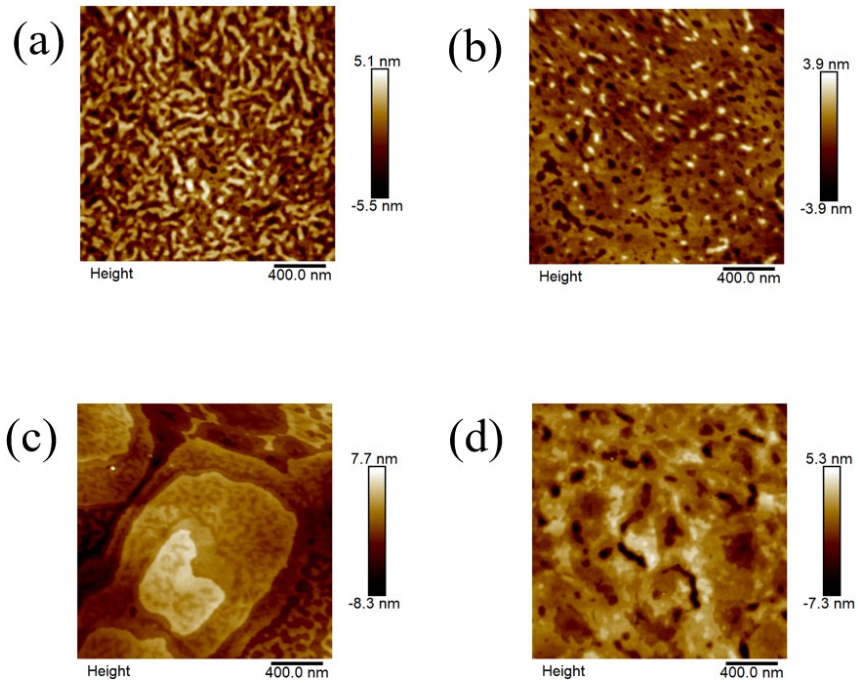

Figure S14. AFM images of thin films based on **PDI-IPD** after multistep annealing at temperature of (a) As, 5 min; (b) 40 ℃; (c) 80 ℃ and (d) 120 ℃, 5 min.

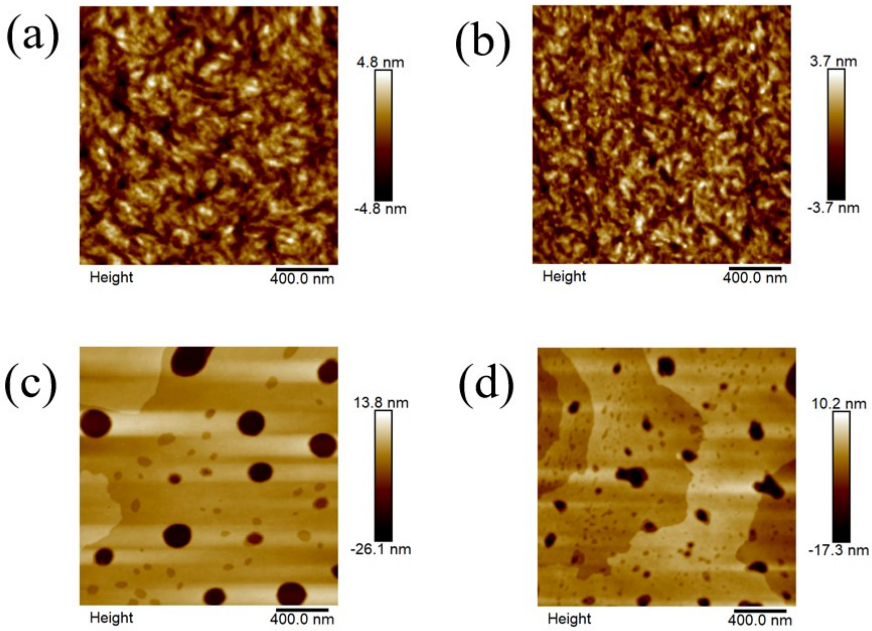

Figure S15. AFM images of thin films based on **PDI-IPZ** after multistep annealing at temperature of (a) As, 5 min; (b) 40 ℃; (c) 80 ℃ and (d) 120 ℃, 5 min.

Phase analysis of X-ray diffraction (XRD)

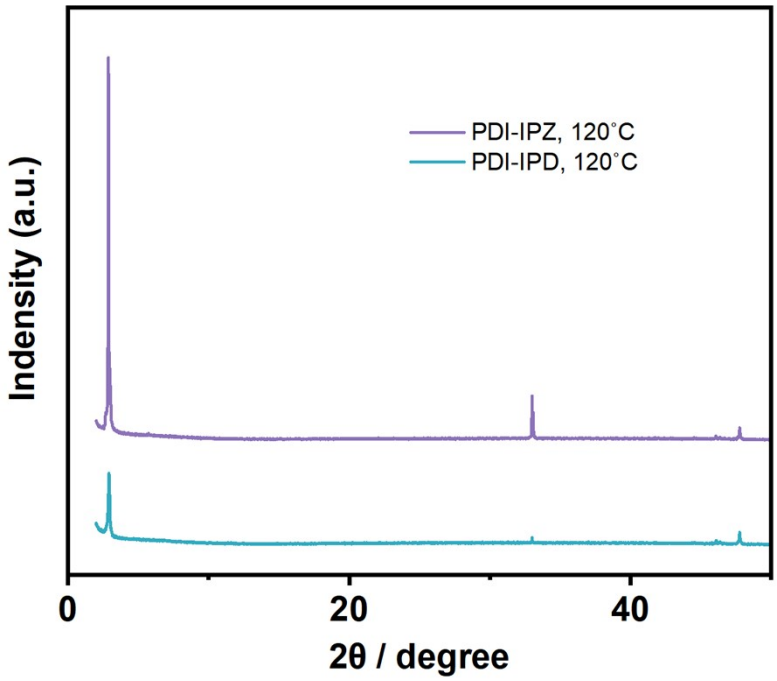

Figure S16. The XRD intensity curves of thin films based on **PDI-IPD** and **PDI-IPZ** after multistep annealing at temperature of 120 ℃, 5 min.